MedChemComm

CONCISE ARTICLE

View Article Online
View Journal | View Issue

Cite this: *Med. Chem. Commun.*, 2015, **6**, 963

New substituted 9-propyladenine derivatives as A_{2A} adenosine receptor antagonists†

C. Lambertucci,[a] M. Buccioni,[a] D. Dal Ben,[a] S. Kachler,[b] G. Marucci,[a] A. Spinaci,[a] A. Thomas,[a] K.-N. Klotz[b] and R. Volpini*[a]

Received 24th January 2015,
Accepted 1st April 2015

DOI: 10.1039/c5md00034c

www.rsc.org/medchemcomm

A new series of 9-propyladenines bearing a phenylalkylamino group in the 2-position or a phenylalkyl chain in the N^6-position, and further substituted with a bromine atom or a 2-furyl ring in the 8-position, were synthesized and tested at human adenosine receptors. The novel compounds proved to be A_{2A} adenosine receptor antagonists and some of them showed high A_{2A} affinity, but moderate selectivity (**18**: K_iA_{2A} = 6.6 nM). Molecular modeling studies gave some explanation of the different activities of the compounds, giving suggestions for the synthesis of new A_{2A} adenosine receptor antagonists.

1. Introduction

The natural nucleoside adenosine (Ado) is the basic constituent of RNA and ATP and, besides that, it interacts with specific receptors belonging to the P1 purinergic receptor family, classified as A_1, A_{2A}, A_{2B}, and A_3 subtypes, which are coupled to G_i (A_1 and A_3) and G_s (A_{2A} and A_{2B}) protein signalling.[1] Adenosine receptors (ARs) are widely distributed in the body, both in the central nervous system (CNS) and the periphery, and regulate many physiological and pathological functions.[2] In fact, there is strong evidence that Ado, through the interaction with its receptors, has a functional role in many diseases ranging from cardiovascular and immune disorders, renal failure and inflammatory conditions to neurological, psychiatric, and neurodegenerative disorders.[3] In the last years, many efforts have been devoted to the synthesis of potent and selective ligands of ARs, and besides that, actually only the A_{2A} selective agonist regadenoson has been approved by the Food and Drug Administration (FDA) and commercialized as Lexiscan (Astellas Pharma Company) for myocardial perfusion imaging.[4] On the other hand, the A_{2A} selective antagonist istradefylline (Nouriast, Kyowa Hakko Kirin Co., Ltd), a novel antiparkinsonian agent, has been approved for manufacturing and marketing at the beginning of 2013 only in Japan.[5,6] Hence, the search for potent and selective ligands of ARs is still a challenge especially for the A_{2B} receptor, which is the last subtype to be pharmacologically characterized due to the lack of selective ligands.[7] In addition to a role in the regulation of mast cell secretion and intestinal functions, the activation of A_{2B} receptors seems to increase fibroblast and endothelial cell migration and to contribute to tissue protection.[8,9] On the contrary, selective antagonists of the A_{2B} receptor could be very useful in the treatment of asthma and allergic diseases since they prevent mast cell degranulation.[10]

In many papers, we have demonstrated that the introduction of diverse substituents in the 2, N^6, 8, and 9-positions of adenine led to AR antagonists endowed with different affinities and selectivities for the four AR subtypes.[11–16] In particular, at human receptors, the 9-ethyladenine (**1**; Fig. 1) resulted in an AR antagonist endowed with μM affinity at the A_1 and A_{2A} subtypes while it was not able to bind the A_{2B} and A_3 receptors at concentrations up to 100 μM (**1**: K_iA_1 = 7400 nM, K_iA_{2A} = 2200 nM).[10]

Introduction of a bromine atom in the 8-position of **1** led to 8-bromo-9-ethyladenine (**2**: Fig. 1), which showed enhanced affinity at all receptor subtypes and resulted in an A_{2A} receptor antagonist endowed with moderate selectivity,

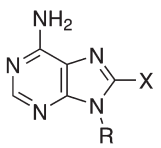

1; R = CH_2CH_3; X = H
2; R = CH_2CH_3; X = Br
3; R = CH_2CH_3; X = 2-Furyl
6; R = $(CH_2)_2CH_3$; X = H
7; R = $(CH_2)_2CH_3$; X = Br
8; R = $(CH_2)_2CH_3$; X = 2-Furyl

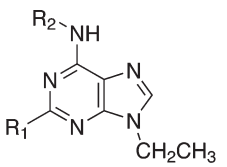

4; R_1 = $NH(CH_2)_2Ph$; R_2 = H
5; R_1 = H; R_2= $(CH_2)_2Ph$

Fig. 1 Known adenine derivatives as antagonists of ARs.

[a] *School of Pharmacy, Medicinal Chemistry Unit, University of Camerino, Via S. Agostino 1, 62032 Camerino, Italy. E-mail: rosaria.volpini@unicam.it*
[b] *Universität Würzburg, Institut für Pharmakologie und Toxikologie, Versbacher Str. 9, 97078, Würzburg, Germany*

† Electronic supplementary information (ESI) available: detailed description of the synthesis and characterization of compounds **12–20**, **22–31**, and **33**; biological assay protocols; computational experiments. See DOI: 10.1039/c5md00034c

especially *versus* the A_1 subtype.[17] The substitution of the bromine atom of **2** with a furyl ring gave a further enhancement of affinity at all ARs, leading again to an A_{2A} antagonist with still moderate selectivity (**3**, Fig. 1; K_iA_{2A} = 3.7 nM, select. A_1/A_{2A} = 6).[15] On the other hand, when a hindered phenethylamino or a phenethoxy group was introduced in the 8-position of **1**, the resulted compounds maintained the A_{2A} selectivity, but were found less active than **2** and **3** at ARs.[11] In the process of investigating substitutions at other positions of the purine core, it was found that the presence of a phenethylamino group in the 2-position of **1** favored the interaction of the resulted compound with all ARs (9-ethyl-2-phenethylaminoadenine, **4**, Fig. 1; K_iA_1 = 330 nM, K_iA_{2A} = 150 nM, K_iA_{2B} = 2410 nM, and K_iA_3 = 3200 nM) while the presence of a phenethyl chain in the N^6-position of **1** gave a compound endowed with enhanced affinity only at the A_{2B} and A_3 subtypes (9-ethyl-N^6-phenethyladenine, **5**: K_iA_1 = 8730 nM, K_iA_{2A} = 1340 nM, K_iA_{2B} = 8130 nM, and K_iA_3 = 10 800 nM). For all these molecules, the further introduction of a bromine atom in the 8-position enhanced the affinity at all ARs. In addition, in a recent paper, we reported that the replacement of the 9-ethyl group of compound **1** with a propyl chain favors the interaction of the resulted compound with the A_{2B} receptors (**6**: K_iA_1 = 9400 nM, K_iA_{2A} = 9600 nM, K_iA_{2B} = 1700 nM, and $K_iA_3 > 100$ μM, Fig. 1, Table 1).[18]

Even in this case, the introduction of a bromine atom or a furyl ring in the 8-position enhanced the affinity of the corresponding compounds **7** and **8** at all ARs. It is worth noting that the 8-bromo-9-propyladenine showed a slight preference for the A_{2B} receptor subtype (**7**: K_iA_1 = 1100 nM, K_iA_{2A} = 300 nM, K_iA_{2B} = 200 nM, and $K_iA_3 \geq 100$ μM).[18]

On these bases, in the search for novel AR antagonists and aimed at investigating the influence of the introduction of a phenylethylamino group in the 2-position or the corresponding phenylethyl chain in the N^6-position combined with a propyl group in the 9-position of adenine, the synthesis of compounds **13** and **24** was undertaken (Fig. 2, Schemes 1 and 2). Furthermore, in order to find the appropriate length of the alkyl chain between the phenyl and the amino group, the ethylene chain was substituted with a methylene or a propylene group (compounds **12**, **14**, **23**, and **25**). In addition, compounds **12–14** and **23–25** were brominated to afford compounds **15–17** and **26–28**, respectively, which were further converted to the corresponding 8-(2-furyl) derivatives **18–20** and **29–31** (Fig. 2, Schemes 1 and 2) as these modifications enhance the affinity of substituted adenine derivatives at ARs.[11,15,17] The new compounds **12–20**, **23–31** were tested in a binding assay at human recombinant A_1, A_{2A}, and A_3 ARs and in the functional cAMP assay at human recombinant A_{2B} ARs. Furthermore, molecular

Table 1 Biological profile of synthesized compounds **12–20** and **23–31** at human adenosine receptors stably transfected in CHO cells

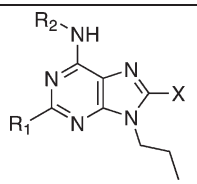

Cpd	R_1	R_2	X	K_iA_1 [a]	K_iA_{2A} [b]	K_iA_{2B} [c]	K_iA_3 [d]
6	H	H	H	9400 (7900–11 000)	9600 (5800–16 000)	1700 (790–3800)	>100 000
7	H	H	Br	1100 (1000–1300)	300 (260–350)	200 (110–380)	>100 000
8	H	H	2-Furyl	19 (13.2–27.4)	18 (8.25–39.4)	252 (167–379)	790 (370–1700)
12	$NHCH_2Ph$	H	H	7600 (5270–11 000)	1400 (931–2120)	>30 000	5840 (4840–7060)
15	$NHCH_2Ph$	H	Br	358 (315–408)	36 (30.7–41.4)	1740 (1154–2630)	650 (471–907)
18	$NHCH_2Ph$	H	2-Furyl	138 (98.8–191)	6.6 (4.19–10.5)	4610 (3910–5430)	29 (20.7–39.4)
13	$NH(CH_2)_2Ph$	H	H	2330 (1840–2950)	738 (609–893)	9250 (6800–12 600)	5880 (5480–6310)
16	$NH(CH_2)_2Ph$	H	Br	373 (289–483)	27 (21.2–34.6)	1490 (1230–1810)	1160 (932–1450)
19	$NH(CH_2)_2Ph$	H	2-Furyl	80 (61.6–105)	14 (11.0–17.7)	2030 (1560–2640)	56 (41.7–74.7)
14	$NH(CH_2)_3Ph$	H	H	3640 (3440–3850)	9110 (7870–10 600)	>30 000	12 600 (11 200–14 100)
17	$NH(CH_2)_3Ph$	H	Br	583 (445–765)	284 (160–502)	6300 (5390–7350)	1950 (1700–2240)
20	$NH(CH_2)_3Ph$	H	2-Furyl	230 (202–261)	113 (87.2–146)	8240 (6700–10 100)	266 (240–294)
23	H	CH_2Ph	H	42 800 (38 900–47 100)	22 600 (13 400–38 100)	>30 000	29 100 (27 400–30 800)
26	H	CH_2Ph	Br	5620 (5060–6230)	1180 (881–1890)	7490 (6820–8240)	11 100 (8010–15 400)
29	H	CH_2Ph	2-Furyl	546 (459–649)	80 (52.7–121)	1760 (1190–2620)	402 (259–625)
24	H	$(CH_2)_2Ph$	H	19 200 (15 900–23 200)	12 000 (7270–19 900)	>30 000	16 900 (16 300–17 600)
27	H	$(CH_2)_2Ph$	Br	1940 (1570–2410)	503 (373–680)	3190 (1890–5400)	2520 (1710–3730)
30	H	$(CH_2)_2Ph$	2-Furyl	2440 (1760–3390)	547 (491–610)	9280 (7170–12 000)	811 (552–1190)
25	H	$(CH_2)_3Ph$	H	18 600 (15 200–22 700)	13 000 (11 900–14 200)	> 30 000	30 000 (24 200–37 400)
28	H	$(CH_2)_3Ph$	Br	2670 (2070–3460)	1020 (872–1190)	1760 (1170–2640)	12 200 (8600–17 200)
31	H	$(CH_2)_3Ph$	2-Furyl	378 (349–408)	181 (137–239)	1870 (986–3550)	959 (812–1130)

[a] Displacement of specific [^{3}H]CCPA binding at human A_1R expressed in CHO cells (n = 3–6). [b] Displacement of specific [^{3}H]NECA binding at human A_{2A}R expressed in CHO cells. [c] K_i values of the inhibition of NECA-stimulated adenylyl cyclase activity in CHO cells expressing human A_{2B} receptors (K_i values were calculated from the corresponding –>IC_{50} values). [d] Displacement of specific [^{3}H]HEMADO binding at human A_3R expressed in CHO cells. Data are expressed as geometric means, with 95% confidence limits.

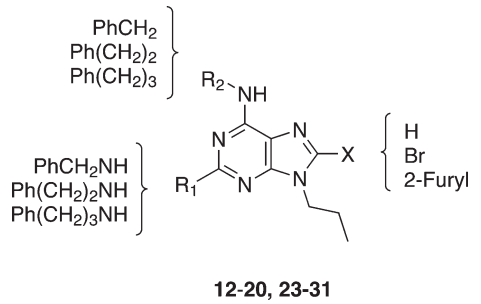

Fig. 2 Structure of designed and synthesized compounds.

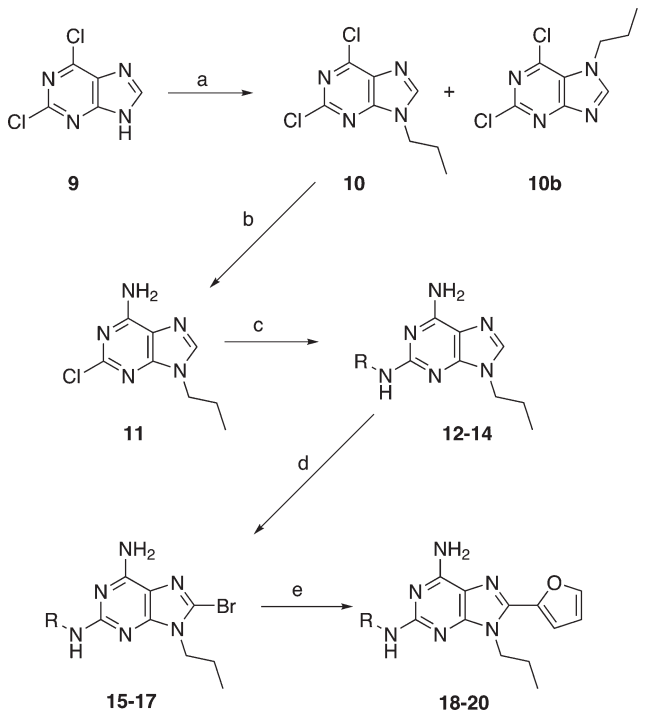

12; 15; 18; R = CH_2-Ph
13, 16; 19; R = $(CH_2)_2$-Ph
14; 17; 20; R = $(CH_2)_3$-Ph

Scheme 1 Synthesis of 2-phenylalkylamino derivatives **12–20**. Reaction conditions: a) Pr-I, K_2CO_3, DMF, rt, 16 h; b) NH_3, rt, 16 h; c) R-NH_2, 120 °C, 24 h; d) NBS, DMF, rt, 1 min; e) (2-tributylstannyl)-furan, $(Ph_3P)_2PdCl_2$, THF, 60 °C, 3 h.

modelling studies have been performed in order to explain the activity of the newly synthesized adenine derivatives.

2. Results and discussion

2.1 Chemistry

Compounds **12–20** and **23–31** were synthesized as summarized in Schemes 1, 2, and 3.

The synthesis of 2-alkylamino-9-propyl derivatives **12–20** was realized by reaction of commercially available 2,6-dichloropurine with propyliodide in the presence of potassium carbonate as previously reported (Scheme 1).[13] After separation of the formed N9 and N7 isomers (**10** and **10a**, respectively) by chromatography, compound **10** was reacted with ammonia to give

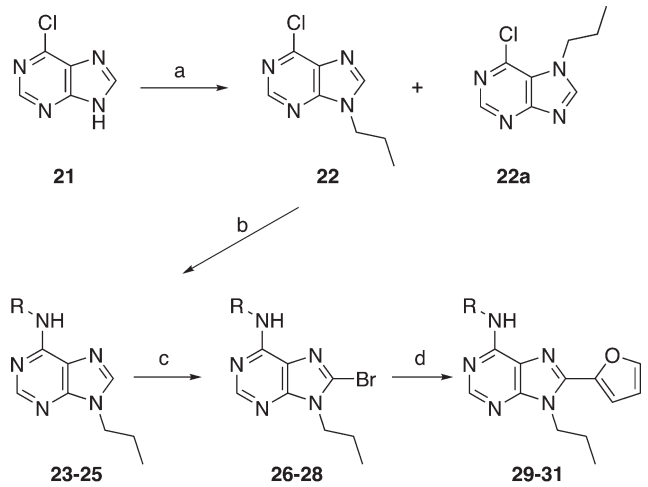

23; 26; 29; R = CH_2-Ph
24; 27; 30; R = $(CH_2)_2$-Ph
25; 28; 31; R = $(CH_2)_3$-Ph

Scheme 2 Synthesis of 6-phenylalkyladenine derivatives **23–31**. Reaction conditions: a) Pr-I, K_2CO_3, DMF, rt, 14 h; b) R-NH_2, 70 °C, 12 h; c) NBS, DMF, rt, 16 h; d) (2-tributylstannyl)furan, $(Ph_3P)_2PdCl_2$, THF, 60 °C, 18 h.

the 6-amino derivative **11**.[13] Reaction of **11** with the suitable amine at 120 °C for 24 h furnished the 2-phenylalkylamino-9-propyl adenines **12–14** with yields ranging from 45 to 88%. Treatment of **12–14** with *N*-bromosuccinimide (NBS), in DMF at room temperature, gave the 8-bromoderivatives **15–17** with yields from 35 to 50%.

Replacement of the 8-bromine atom with a 2-furyl ring was obtained by reaction of compounds **15–17** with (2-tributylstannyl)furan using triphenylphosphine palladium(II) chloride as catalyst and anhydrous THF as solvent (Scheme 1).

After 3 h at 60 °C the reactions were complete; the 8-(2-furyl) derivatives **18–20** were obtained in 55–70% yield. Compounds **23–31** were synthesized by reacting commercially available 6-chloropurine with propyliodide in anhydrous DMF in the presence of potassium carbonate (Scheme 2). The reaction was previously reported using propylbromide and in that case only the N9 isomer was described. In the present case also the N7 isomer was detected and described.[19] The reaction was conducted at room temperature and yielded the N9, **22**, and N7, **22a**, isomers (64 and 28%, respectively) after column chromatography. The two isomers were characterized by a comparison of NMR data with analogue purine

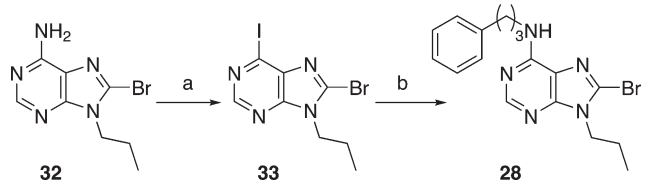

Scheme 3 Synthesis of 8-bromo-6-phenylpropyladenine (**28**). Reaction conditions: a) i-$C_5H_{11}ONO$, CH_2I_2, CH_3CN, 85 °C, 30 min; b) R-NH_2, 70 °C, 12 h.

derivatives.[13,17] In fact, the N-9 alkylated adenines showed an upfield shift of the H-8 and NH_2 protons with respect to the same protons of the N-7 isomers. Furthermore, the N-9 isomers are always obtained in higher yields and show lower polarity in the TLC run such as in compounds **22** with respect to **22a**. Reaction of **22** with the suitable amine, in the presence of 4-(dimethylamino)pyridine (DMAP) in anhydrous acetonitrile at 70 °C for 12 h, furnished the 6-phenylalkyl-9-propyladenine derivatives **23–25** with yields ranging from 58 to 92% (Scheme 2). Treatment of the latter compounds with NBS in DMF at room temperature gave **26** and **27** with yields of 19 and 38%, respectively, while only a few milligrams of the impure compound **28** were obtained. Hence, a different synthetic pathway has been chosen to obtain this compound, as depicted in Scheme 3. To this purpose, the 8-bromo-9-propyladenine (**32**)[17] was treated in Sandmeyer's conditions with isoamyl nitrite and diiodomethane at 60 °C to give the 8-bromo-6-iodo-9-propyl-adenine (**33**) in 54% yield. Compound **33** was then reacted with 3-phenylpropylamine at 60 °C for 4 h to give **28** in 53% yield.

The 8-bromoadenine derivatives **26–28** were used to prepare the 8-furyladenine analogues **29–31** as previously described, but for a longer time (Scheme 2).

In fact, by reaction of compounds **26–28** with (2-tributylstannyl)furan, in the presence of bis(triphenylphosphine) palladium(II) dichloride, in anhydrous THF at 60 °C for 18 h, the 8-furyladenine derivatives **29–31** were obtained.

2.2 Biological activity

Compounds **12–31** were tested in a radioligand binding assay at human recombinant ARs, expressed in Chinese hamster ovary (CHO) cells, in order to evaluate their affinity at A_1, A_{2A}, and A_3 AR subtypes using as radioligands [^{3}H]CCPA (2-chloro-N^6-cyclopentyl-adenosine), [^{3}H]NECA (5′-*N*-ethylcarboxamidoadenosine), and [^{3}H]HEMADO (2-hexyn-2-yl-N^6-methyladenosine), respectively.[20,21] The results are reported as K_i values nM, with 95% confidence intervals in parentheses (Table 1). At A_{2B} receptors, K_i values were calculated from IC_{50} values determined by inhibition of NECA-stimulated adenylyl cyclase activity (Table 1).[20] Previously, it has been reported that the replacement of the ribose moiety of adenosine nucleosides with alkyl groups led to compounds which lose the intrinsic activity and behave as AR antagonists;[12,22] for this reason the newly synthesized series of compounds are believed to be antagonists of ARs and they have been characterized only with the radioligand binding assay.

The 9-propyladenine (**6**), together with its 8-bromo and 8-furylderivatives **7** and **8**, were reported as reference compounds.[18] Most of the newly synthesized derivatives displayed K_i values ranging from μM to low nM concentrations at ARs and all of them resulted in A_{2A} antagonists without relevant selectivity, especially *versus* the A_1 and A_3 AR subtypes. At A_{2B} receptors, the new substituted 9-propyladenine derivatives **12–31** showed lower affinity than the unsubstituted parent compound 9-propyladenine (**6**: K_iA_{2B} = 1700 nM) and, obviously, than the corresponding 8-bromo and 8-furyl derivatives **7** (K_iA_{2B} = 200 nM) and **8** (K_iA_{2B} = 250 nM). Moreover, they were inactive when unsubstituted in the 8-position (see compounds **12–14** and **24**, **25**: $K_iA_{2B} > 30$ μM), with the exception of the 2-phenethylamino-9-propyladenine (**13**) which displayed a K_iA_{2B} of 9250 nM. On the other hand, the corresponding derivatives, bearing a bromine atom or a furyl ring in the 8-position (compounds **15–20** and **26–31**), were able to activate the A_{2B} receptor subtype but at concentration in the μM range, so resulting in all cases less active than the 8-bromo-9-propyladenine (**7**: K_iA_{2B} = 200 nM) and the 8-furyl-9-propyladenine (**8**: K_iA_{2B} = 250 nM). These data clearly indicate that the combination of a propyl chain in the 9-position of adenine with a phenylalkylamine in the 2-position or a phenylalkyl chain in the N^6-position does not favor the interaction of the corresponding derivatives with A_{2B} receptors.

In addition, the presence of a phenylalkyl chain in the N^6-position of **6** led to the same results also at A_1 and A_{2A} AR subtypes; in fact, compounds **23–25** were found less active than **6** at these receptors, as well as the corresponding 8-bromo and 8-furyl derivatives **26–28** and **29–31**, respectively, compared to the 8-bromo-9-propyladenine (**7**: K_iA_1 = 1100 nM and K_iA_{2A} = 300 nM) and the 8-furyl-9-propyladenine (**8**: K_iA_1 = 19 nM and K_iA_{2A} = 18 nM). However, the N^6-benzyl-8-furyl-9-propyladenine (**29**) is the most active ligand, among this series, at the A_{2A} receptor with K_i = 80 nM. Conversely, the introduction of the phenylalkyl chain in the N^6-position of **6** seems to favor the binding at A_3 receptors (**23**: K_iA_3 = 29 100 nM; **24**: K_iA_3 = 16 900 nM; and **25**: K_iA_3 = 30 000 nM *vs.* **6**: $K_iA_3 > 100$ μM). As expected, the further introduction of a bromine atom or a furyl ring in the 8-position gave an increase in A_3 affinity; the 8-furyl derivatives **29–31** are the most active in the series of the N^6-substituted derivatives. Also at the A_3 receptor subtype compound **29** showed the better affinity profile of this series, with a K_i slightly lower than **8** (**29**: K_iA_3 = 402 nM *vs.* **8**: K_iA_3 = 790 nM). The best results were obtained with the series of the 2-substituted derivatives. In fact, compounds **12–20** were found in general to be more active at A_1, A_{2A} and A_3 ARs than the corresponding 2-unsubstituted derivatives **6–8**. An exception is represented by the 8-furyl derivatives **18–20** at A_1 receptors (K_i values ranging from 80 to 238 nM *vs.* **8**: K_iA_1 = 19 nM) and **20** at the A_{2A} receptor subtype, which was less active than **8** (**20**: K_iA_{2A} = 113 nM *vs.* **8**: K_iA_{2A} = 18 nM). It is worthwhile to note that the 2-benzylamino-8-furyl-9-propyladenine was more active than the 8-furyl-9-propyladenine at A_{2A} and A_3 receptors (**18**: K_iA_{2A} = 6.6 nM and K_iA_3 = 29 nM *vs.* **8**: K_iA_{2A} = 18 nM and K_iA_3 = 790 nM) and behaved as the most active compound among the two new series of 9-propyladenine derivatives at the same receptor subtypes.

2.3 Molecular modelling analysis

On the basis of the biological results, we decided to perform a molecular modelling analysis to better understand the

different interactions of the synthesised molecules with $A_{2A}AR$. In particular, molecular docking methods were employed to simulate the interaction of compounds **12–20** and **23–31** with the binding site of the human $A_{2A}AR$ crystal structures solved in the complex with ZM241385 antagonist (Protein Data Bank -pdb- code: 3EML; 2.6 Å resolution[23,24]). The crystal structure was re-modelled by firstly removing the external T4L segment and secondly by performing a building of missing receptor regions (the missing section of the extracellular 2 -EL2- or intracellular 3 -IL3- domains). The obtained $A_{2A}AR$ model was checked by using the Protein Geometry Monitor application within the Molecular Operating Environment (MOE, version 2010.10) suite,[25] which provides a variety of stereochemical measurements for structural quality inspection in a given protein, such as backbone bond lengths, angles and dihedrals, Ramachandran φ–ψ dihedral plots, and sidechain rotamer and nonbonded contact quality.

The $A_{2A}AR$ structure was then used as a target for the docking analysis of synthesised derivatives.

All ligand structures were optimized using RHF/AM1 semi-empirical calculations and the MOPAC software package implemented in MOE was utilized for these calculations.[26] The compounds were then docked into the binding site of the $A_{2A}AR$ model by using the MOE Dock tool. Docking poses of each compound were subjected to energy minimization and then rescored using three available methods implemented in MOE: the *London dG* scoring function that estimates the free energy of binding of the ligand from a given pose; the *Affinity dG* scoring tool that estimates the enthalpic contribution to the free energy of binding; the *dock*-pK_i predictor that uses the MOE *scoring.svl* script to estimate for each ligand a pK_i value, which is described by the H-bond, transition metal interaction, and hydrophobic interaction energy. For each compound, the top-score docking poses at the $A_{2A}AR$ model, according to at least two out of three scoring functions, were selected for final ligand–target interaction analysis. The docking methodology was firstly tested by comparing the predicted binding mode of ZM241385 within the $A_{2A}AR$ pocket with respect to the X-ray data. The docking method showed good ability in reproducing the ZM241385 binding mode observed in the experimental data. In particular, the Root Mean Square Deviation (RMSD) from the comparison of the crystal structure and the docking conformation was calculated to be 1.45 Å.

The 2-substituted 9-propyladenine derivatives present structural similarities with the ZM241385 compound and the docking results show for these new molecules a general binding mode comparable to that of the $A_{2A}AR$ reference ligand (observed at the 3EML crystal structure) and observable in Fig. 3. In detail, the compound adenine scaffold is almost vertically oriented and located between residues of the TM3 (Phe168) and TM6 (Leu249) domains, in a similar fashion to the purine position and orientation observed from the binding mode of the nucleoside Ado within the $hA_{2A}AR$ crystal structure (pdb code: 2YDO[27]) and analogously to other adenine derivatives previously analysed at a $hA_{2A}AR$ model.[15,18]

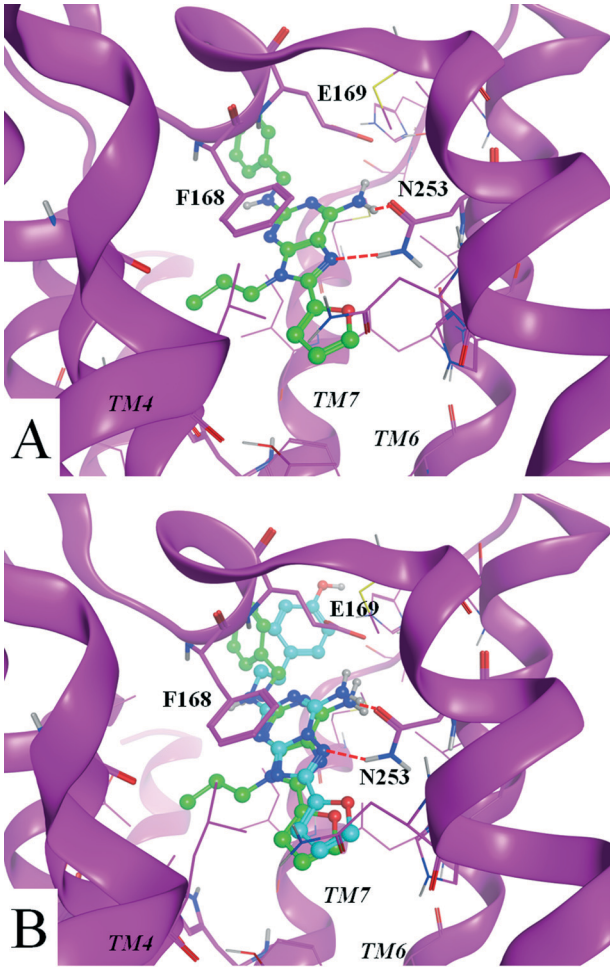

Fig. 3 Binding modes at $hA_{2A}AR$ of the 2-substituted adenine derivatives. The docking conformation of compound **18** (green) is shown as obtained by the docking analysis (A) or as superimposed to the original binding mode of the co-crystallized compound ZM241385 (cyan). (B) Some key residues are indicated within the figure. Polar interactions (*i.e.* with N253) are indicated with red dashed lines.

The 6-amino group and the N7 nitrogen atom give a double H-bond interaction with the TM6 Asn253 residue. The 8-position pointing towards the receptor core is located between residues of TM3 (Leu85, Thr88), TM5 (Met177), and TM6 (Trp246, His250, Leu249) segments, while the 9-propyl group is located between residues of TM3 (Leu85), TM5 (Met177), and TM6 (Trp246) domains. The oxygen atom of the furyl ring inserted in the 8-position could provide an additional H-bond interaction to Asn253, analogous to what is observed for the $hA_{2A}AR$–ZM241385 complex from the crystal structure employed in this study. This data could explain the higher affinity of the 8-furyl substituted analogues than the corresponding 8-bromo or 8-unsubstituted derivatives. The 2-substituent points toward the extracellular space. Results of binding studies report that the length of the alkyl spacer of the 2-substituent provides higher affinity if it is among 1 and 2 carbon atoms, while a propyl spacer seems generally detrimental for the binding activity. The binding mode suggested by the docking results presents the phenyl ring of the

2-substituent as well inserted between EL2 and EL3 residues only in the presence of a methyl or ethyl spacer within this substituent, while a propyl linker makes the phenyl ring more externally located and hence exposed to the solvent. This could be the factor explaining the different compound affinity based on the diverse length of the 2-group.

Considering the N^6-substituted 9-propyladenine derivatives, docking results allowed to identify two families of binding modes. The first family (Fig. 4A), selected considering the docking conformations with the highest scores from two out of three scoring functions, presents the compound adenine scaffold located between residues of the transmembrane TM3 (Phe168) and TM6 (Leu249) domains. The purine moiety is vertically oriented with the 8-position pointing towards the receptor core and the 6-amino group positioned nearby the TM2-TM3 amino acids. The N3 nitrogen atom is located in proximity to the TM6 residues, providing H-bond interaction with the polar hydrogen atoms of the Asn253 sidechain.

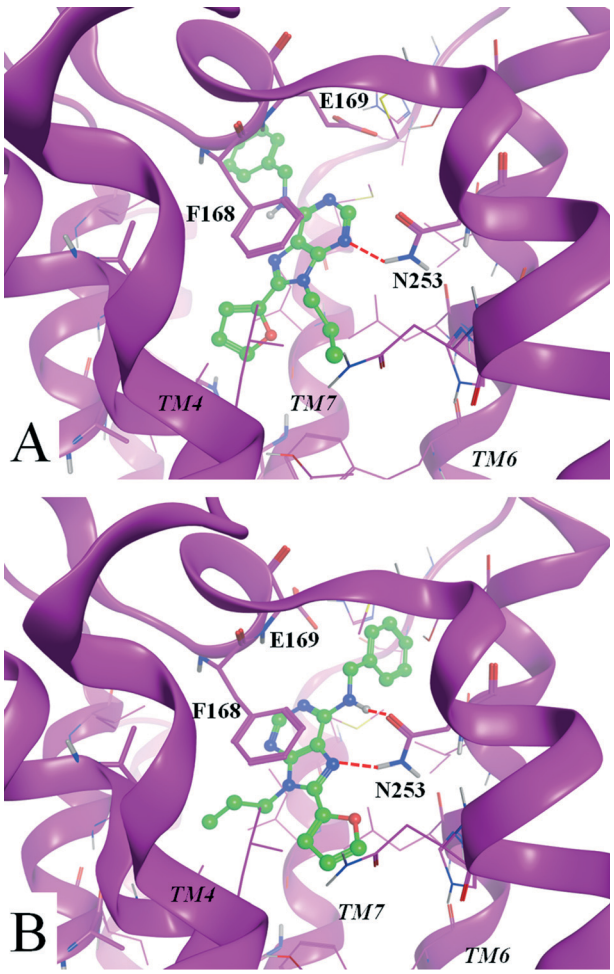

Fig. 4 Binding modes at $hA_{2A}AR$ of the N^6-substituted adenine derivatives. Family 1 (A) and family 2 (B) docking conformations of compound **29** are displayed. The ligand is coloured green. Some residues are indicated within the figure. Polar interactions (*i.e.* with N253) are indicated with red dashed lines.

The 9-propyl chain is positioned in a sub-cavity given by residues belonging to the TM3 (Leu85, Thr88), TM5 (Met177), and TM6 (Trp246, His250, Leu249) domains and presenting mainly a hydrophobic profile. The 8-substituent gets in proximity to residues of TM2 (Ala63), TM3 (Val84, Leu85), TM6 (Trp246), and TM7 (Ile274, Ser277, His278).

The furyl ring inserted in this position seems to better fill the sub-pocket given by the above cited residues with respect to the bromine atom and a potential H-bond interaction between the oxygen atom of the furyl ring and the hydroxyl function of the Ser277 (TM6) sidechain is observable. In this sense, docking results could explain why the compounds with a 8-furyl substituent present in general a higher $hA_{2A}AR$ affinity with respect to the 8-bromo analogues, considering at least the compounds presenting a benzyl or a phenylpropyl group in the N^6-position. The N^6-substituent points toward the extracellular space and is located between residues belonging to TM2 (Ala63, Ile66), EL2 (Leu167), and TM7 (Met270, Tyr271) residues.

This substituent is hydrophobic and the interaction with the nearby residues is nonpolar. The different length of the spacer (methyl to propyl linker) has a significant impact on the affinity for the $A_{2A}AR$; in this sense, considering these docking conformations, the different length of the linker could have a modulating effect on the flexibility of the N^6-substituent and hence on its easy or difficult fitting within the binding cavity.

The second family of binding modes contains conformations whose scores present the most similar trend compared to the compound pK_i values. These conformations are also endowed with the highest scores according to one of the scoring functions (*London dG*). This binding mode (Fig. 4) presents the compound adenine scaffold positioned and oriented in a similar fashion than the docking conformations of the 2-substituted derivatives, with the purine moiety located between residues of the TM3 (Phe168) and TM6 (Leu249) domains. This binding mode allows again the observation of a double H-bond interaction between the 6-amino group and the N7 nitrogen atom and the TM6 Asn253 residue, the 8- and 9-substituents pointing toward the receptor core and located between residues of TM3, TM5, and TM6 segments, and the oxygen atom of the furyl ring inserted in the 8-position providing an additional H-bond interaction to Asn253. The N^6-substituent points towards the extracellular space and is positioned and oriented similarly to the first family of docking conformations, even if more in proximity to the TM6-EL3 residues. Taking together the results of the N^6-substituted derivatives, both the above described docking conformations provide two possible binding modes that may explain in different ways the higher activity of the 8-furyl substituted derivatives, while the length of the N^6-substituent alkyl chain seems to modulate the affinity providing different flexibility to the whole substituent.

A comparison of the docking conformations of the 2- and N^6-substituted derivatives was made by superimposition within the MOE interface (Fig. 5). The first family of docking

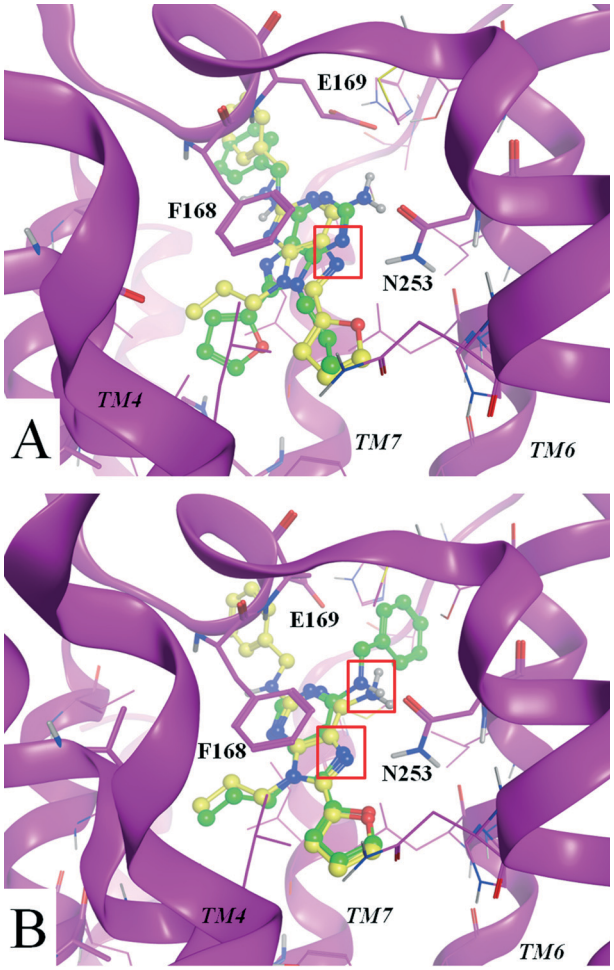

Fig. 5 Comparison of the binding modes at $hA_{2A}AR$ of the 2- and N^6-substituted adenine derivatives (**18**, yellow, and **29**, green, respectively). Superimposition of the binding modes of the 2-substituted derivatives with the first family of docking conformations of N^6-substituted adenines (A) highlights the analogue position of the phenylalkyl chains and the matching of the 8-substituent of the first group of molecules with the 9-substituent of the second group of compounds and *vice-versa*. Superimposition of the binding modes of the 2-substituted derivatives with the second family of docking conformations of N^6-substituted adenines (B) highlights the match of the purine scaffolds and the 8- and 9-substituents, while the phenylalkyl chains of the two series of molecules are differently located within the binding cavity. Red squares indicate the matching of H-bond acceptors or donors in proximity to the N253 residue.

conformations of the N^6-substituted derivatives presents the purine moiety oriented in a mirrored fashion with respect to the same scaffold of the 2-substituted compounds. This feature makes the N^6-substituent of the first group of molecules to be located and oriented similarly to the analogue group of the 2-substituted compounds. Interestingly, the 8-substituent of the first group of molecules is positioned in correspondence to the 9-substituent of the second group of compounds and *vice-versa*. The N3 atom of the N^6-substituted derivatives is similarly located at the N7 atom of the 2-substituted molecules and both atoms provide H-bond interaction with the Asn253 sidechain. The H-bond donor feature given by the 6-amine of the 2-substituted adenines is unoccupied by an analogue group of the N^6-substituted derivatives. This data could explain the higher affinity of the 2-substituted derivatives. Hence, a possible modification of the N^6-substituted adenines by insertion of an amine group in the 2-position seems to be suggested by the docking results. The second family of docking conformations of the N^6-substituted adenines presents the purine moiety quite perfectly matching with the same scaffold of the 2-substituted compounds, with the 8- and 9-substituents of the two series occupying analogue positions. In this sense, the different position occupied by the phenyl-alkyl substituents could be the factor explaining the different binding activity of the two series of compounds.

Conclusions

In this work, two new series of 9-propyladenine derivatives substituted at the 2-position with phenylalkylamino chains and at the N^6-position with phenylalkyl chains of different lengths were synthesized and tested at ARs in a radioligand binding assay (A_1, A_{2A}, and A_3 AR subtypes) and evaluated for their ability to modulate the adenylyl cyclase activity (A_{2B} ARs). Biological data for the new compounds showed that the presence of a propyl chain, in the N9-position of the purine moiety, combined with a phenylalkylamine in the 2-position or a phenylalkyl chain in the N^6-position does not improve affinity at A_{2B} ARs as it could be hypothesized. In fact, both the N^6- and the 2-substituted 9-propyladenine derivatives (**12–20** and **23–31**, respectively) were A_{2A} AR antagonists endowed with moderate selectivity, although in some cases the compounds showed a high A_{2A} affinity in the low nM range. In particular, the 2-benzylamino-8-furyl-9-propyladenine (**18**) was more active than the parent 8-furyl-9-propyladenine at A_{2A} and A_3 ARs (**18:** K_iA_{2A} = 6.6 nM and K_iA_3 = 29 nM *vs.* **8:** K_iA_{2A} = 18 nM and K_iA_3 = 790 nM). Molecular modeling studies gave some explanation of the different activities of the compounds at the A_{2A} AR. This study contributed to strengthen the finding that the introduction of a phenylalkylamino chain in the 2 and 6 positions of 9-alkyl purine derivatives favors the interaction of the resulted compounds with the A_{2A} AR subtype giving suggestions for the synthesis of new antagonists of this receptor.

Acknowledgements

This work was supported by Fondo di Ricerca di Ateneo (University of Camerino) and by a grant from the Italian Ministry for University and Research (PRIN2010-11 no 20103W4779_003).

Notes and references

1 B. B. Fredholm, A. P. IJzerman, K. A. Jacobson, J. Linden and C. E. Muller, *Pharmacol. Rev.*, 2011, **63**, 1–34.
2 K. A. Jacobson and Z. G. Gao, *Nat. Rev. Drug Discovery*, 2006, **5**, 247–264.

3 C. N. Wilson and S. J. Mustafa, *Handb. Exp. Pharmacol.*, 2009, v–vi.
4 C. E. Muller and K. A. Jacobson, *Biochim. Biophys. Acta*, 2011, **1808**, 1290–1308.
5 R. Dungo and E. D. Deeks, *Drugs*, 2013, **73**, 875–882.
6 S.-I. Uchida, K. Soshiroda, E. Okita, M. Kawai-Uchida, A. Mori, P. Jenner and T. Kanda, *Eur. J. Pharmacol.*, 2015, **747**, 160–165.
7 R. Volpini, S. Costanzi, S. Vittori, G. Cristalli and K.-N. Klotz, *Curr. Top. Med. Chem.*, 2003, **3**, 427–443.
8 C. M. Aherne, E. M. Kewley and H. K. Eltzschig, *Biochim. Biophys. Acta*, 2011, **1808**, 1329–1339.
9 I. Feoktistov, I. Biaggioni and B. N. Cronstein, *Handb. Exp. Pharmacol.*, 2009, 383–397.
10 A. Mohsenin and M. R. Blackburn, *Curr. Opin. Pulm. Med.*, 2006, **12**, 54–59.
11 E. Camaioni, S. Costanzi, S. Vittori, R. Volpini, K.-N. Klotz and G. Cristalli, *Bioorg. Med. Chem.*, 1998, **6**, 523–533.
12 K.-N. Klotz, S. Kachler, C. Lambertucci, S. Vittori, R. Volpini and G. Cristalli, *Naunyn-Schmiedeberg's Arch. Pharmacol.*, 2003, **367**, 629–634.
13 C. Lambertucci, G. Cristalli, D. Dal Ben, D. D. Kachare, C. Bolcato, K.-N. Klotz, G. Spalluto and R. Volpini, *Purinergic Signalling*, 2007, **3**, 339–346.
14 C. Lambertucci, S. Vittori, R. C. Mishra, D. Dal Ben, K.-N. Klotz, R. Volpini and G. Cristalli, *Nucleosides, Nucleotides Nucleic Acids*, 2007, **26**, 1443–1446.
15 R. Volpini, D. Dal Ben, C. Lambertucci, G. Marucci, R. C. Mishra, A. T. Ramadori, K.-N. Klotz, M. L. Trincavelli, C. Martini and G. Cristalli, *ChemMedChem*, 2009, **4**, 1010–1019.
16 C. Lambertucci, M. Buccioni, B. Cacciari, D. Dal Ben, S. Federico, K.-N. Klotz, G. Marucci, R. Volpini, G. Spalluto and G. Cristalli, *Collect. Czech. Chem. Commun.*, 2011, **76**, 1379–1393.
17 C. Lambertucci, I. Antonini, M. Buccioni, D. Dal Ben, D. D. Kachare, R. Volpini, K.-N. Klotz and G. Cristalli, *Bioorg. Med. Chem.*, 2009, **17**, 2812–2822.
18 D. Dal Ben, M. Buccioni, C. Lambertucci, A. Thomas, K.-N. Klotz, S. Federico, B. Cacciari, G. Spalluto and R. Volpini, *Eur. J. Med. Chem.*, 2013, **70C**, 525–535.
19 G. D. Celik, A. Disli, Y. Oner and L. Acik, *Med. Chem. Res.*, 2013, **22**, 1470–1479.
20 K.-N. Klotz, J. Hessling, J. Hegler, C. Owman, B. Kull, B. B. Fredholm and M. J. Lohse, *Naunyn-Schmiedeberg's Arch. Pharmacol.*, 1998, **357**, 1–9.
21 K.-N. Klotz, N. Falgner, S. Kachler, C. Lambertucci, S. Vittori, R. Volpini and G. Cristalli, *Eur. J. Pharmacol.*, 2007, **556**, 14–18.
22 R. D. Thompson, S. Secunda, J. W. Daly and R. A. Olsson, *J. Med. Chem.*, 1991, **34**, 2877–2882.
23 V. P. Jaakola, M. T. Griffith, M. A. Hanson, V. Cherezov, E. Y. Chien, J. R. Lane, A. P. IJzerman and R. C. Stevens, *Science*, 2008, **322**, 1211–1217.
24 D. Dal Ben, C. Lambertucci, G. Marucci, R. Volpini and G. Cristalli, *Curr. Top. Med. Chem.*, 2010, **10**, 993–1018.
25 Molecular Operating Environment; C.C.G., Inc., 1255 University St., Suite 1600, Montreal, Quebec, Canada, H3B 3X3.
26 J. J. Stewart, *J. Comput.-Aided Mol. Des.*, 1990, **4**, 1–105.
27 G. Lebon, T. Warne, P. C. Edwards, K. Bennett, C. J. Langmead, A. G. Leslie and C. G. Tate, *Nature*, 2011, **474**, 521–525.

